



Corundum inclusions in diamonds—discriminatory criteria and a corundum compositional dataset[☆]

Mark T. Hutchison^{a,b,*}, Peter H. Nixon^c, Simon L. Harley^d

^a Lunar and Planetary Laboratory, University of Arizona, Tucson, AZ, USA

^b Research School of Earth Sciences, Australian National University, Canberra, ACT 0200, Australia

^c University of Leeds, Leeds, UK

^d University of Edinburgh, Edinburgh, UK

Received 27 June 2003; accepted 14 December 2003

Available online 1 June 2004

Abstract

Mineral inclusions of corundum are reported from diamonds from alluvial deposits of tributaries of the Rio Aripuanã, Juina, Brazil. We present the first recorded occurrence of sapphire as an inclusion in diamond and expand on the database of ruby and white corundum inclusions. Ruby inclusions are found to occur both as isolated and touching grains with aluminous pyroxene and associated with ferropicriolite. Mineral chemistry and phase relations place the origin of such ruby-bearing diamonds within the lower mantle at ~ 770 km. Mineral associations involving other corundum inclusions were not observed; hence, their depth of origin is less certain.

Compositions of corundum samples were characterised by electron and ion microprobe. Given the scarcity of literature data, corundum samples from a variety of other geological settings were also analysed. Samples comprised corundums associated with granitic emplacement, metasomatism, amphibolite-facies and granulite-facies rocks, gem and industrial synthetic origins and carmine-coloured corundums recovered from kimberlite drill cores.

In addition to variable amounts of Cr, Fe, Ti, Mg and Si, measurable quantities of other transition elements and high field strength elements were also detected. Corundums from similar geological settings show very similar compositions and are easily distinguishable from other settings. Irrespective of locality, rubies from Norwegian, Tanzanian and Kenyan amphibolite-facies rocks are compositionally indistinguishable. Additionally, corundums from metasomatised zones associated with contact metamorphism from Arizona and Japan were very similar, particularly characterised by unusually high abundance of mobile Zr and Nb (tens of ppm). All Juina inclusions are particularly distinguishable from other corundums by high concentrations of Ni (18–171 ppm weight), typically at least an order of magnitude enriched over the same corundum varietal types from elsewhere. Furthermore, the sapphire inclusion exhibited much larger ratios of Ga and Ge to HFSE elements compared to otherwise similar samples, and ruby inclusions are distinguished by high Mg/Fe ratios (0.27–1.56 by weight). Compositional differences between inclusions in diamonds and corundums from other settings in

[☆] Supplementary data associated with this article can be found, in the online version, at [doi:10.1016/j.lithos.2004.04.006](https://doi.org/10.1016/j.lithos.2004.04.006).

* Corresponding author. Research School of Earth Sciences, Australian National University, Mills Road, Canberra ACT 0200, Australia.
E-mail address: mhutchis@lpl.arizona.edu (M.T. Hutchison).

addition to corundum's physical and chemical durability suggest that with the employment of rapid identification tools such as energy dispersive spectrometry (EDS) and laser-ICPMS, corundum has promise as an indicator of diamond prospectivity.

© 2004 Elsevier B.V. All rights reserved.

Keywords: Corundum; Diamond inclusion; Mantle; Trace element; Nickel

1. Introduction

Corundum has been previously reported as occurring as syngenetic inclusions in diamonds from the alluvial deposits of tributaries of the Rio Aripuanã, Juina, Brazil (Watt et al., 1994; Hutchison et al., 2001). Diamonds from this area are of particular interest as they contain the most comprehensive source of deep transition zone and lower mantle material available for study (Hutchison, 1997; Harte et al., 1999; Gasparik and Hutchison, 2000; Hutchison et al., 2001). Here we report the first occurrence of corundum var. sapphire as a syngenetic inclusion in diamond and present data for white corundum inclusions from the same source. We also expand upon the first description of corundum var. ruby occurring as part of a mineral association within diamond (Hutchison et al., 2001) and reflecting a lower mantle origin. By studying the geochemistry of corundum inclusions, we aim to provide further insights into characteristics that discriminate the deep mantle from other more commonly observed sources of corundum.

Corundum is often observed by prospectors in alluvial settings in association with diamond (Mousseau Tremblay, personal communication, 2002). Given the range of common rock types in which corundum can occur, its existence in heavy mineral separates is perhaps not surprising. However, the identification of corundum inclusions within diamonds supports at least an occasional genetic link. As corundum is also resistant to weathering, the propensity exists to use this mineral as an indicator for diamond prospectivity. For corundum to be useful for this purpose, however, means must be established to isolate corundums with a diamond affinity from those from other mantle and crustal sources.

Despite the low abundances of trace elements in corundums, they do contain measurable quantities. Furthermore, because the Al_2O_3 structure contains sites appropriate for hosting high field strength ele-

ments and a number of transition metals that are fractionated in widely differing fashions in different mantle and crustal settings, trace elements could provide a means of identifying corundums grown in different settings. Here we present preliminary discriminatory tools for corundum genesis on the basis of minor and trace element data.

Although quantitative analyses of corundums do appear in the literature, data presented are most commonly routine electron microprobe (EPMA) analyses where trace element data is not available and minor element analyses are subject to large errors. Precision trace element data for corundums occur only sparsely (Schreyer et al., 1981; Kerrich et al., 1987; Limtrakun et al., 2001; Emmet et al., 2003). To supplement available data, we have collected and analysed corundums from a variety of source environments in addition to inclusions in diamonds. Samples associated with granitic emplacement were procured in addition to those from amphibolite-facies and granulite-facies rocks, and various synthetic origins. Finally, carmine-coloured corundum grains from kimberlite drill cores from Saskatchewan, Canada, were included in the sample set. Secondary ion mass spectrometry (SIMS) was used for trace element analyses; however, to obtain absolute concentration data, it was also necessary to fabricate and characterise appropriate standards.

2. Corundum inclusions in diamonds

Corundum-occluding diamonds were collected from a wide area of alluvial gravels from the Juina district of Mato Grosso, Brazil, centred on $-59^{\circ}05'50''$ West, $-11^{\circ}23'33''$ South, which corresponds to (271015, 8736200) on Brazilian 1:250 000 Map SC21-Y-C (Juina). The samples came from the Rio Vinte e Um and the Rio Cinta Larga and its tributaries the Rio Mutum, Igarapé Porcão, Rio Juini-

nha and Rio Juina-Mirim. Diamonds from this area are the subject of a number of previous publications (Harris et al., 1997; Harte et al., 1999; Hutchison et al., 1999, 2001) and thesis work of Hutchison (1997). Observations have been repeated on similar samples from the same area more recently by Kaminsky et al. (2001). Kimberlitic sources of these diamonds have not so far been identified; however, anomalous electromagnetic signatures and an abundance of kimberlitic ilmenites and G9 garnets in associated gravels suggests diamonds were recovered close to their source rocks. Furthermore, Diagem International Resources Corp. have recently discovered kimberlite in a different catchment area approximately 8 km away from the present source area. The corundum inclusions were recovered from their host diamonds by fracturing in a purpose-built steel anvil as described below.

Table 1 details the occurrence of corundum inclusions in Juina diamonds and summarises the mineralogy and geochemistry of diamond hosts and associated mineral inclusions. Three inclusions of ruby have been recovered with one 60- μm sample (BZ241C) being a touching grain with a high-Al (10 wt.%) Mg-pyroxene (BZ241B1). This composite inclusion was recovered from within the same diamond as a syngenetic inclusion of ferropicroclase [(Mg,Fe)O]. The other two ruby inclusions are a small grain released from the same diamond and the separate ruby sample of Watt et al. (1994). Additionally, a single 300- μm intense blue sapphire inclusion and two white corundums were

recovered from three separate diamonds. A colour photograph of sample BZ241B1,C polished and mounted within epoxy and taken in transmitted light is available from the supplementary data set.

Where analysed, occluding diamonds are Type IIa, which means that they have subdetection-level (~ 15 ppm) concentrations of nitrogen (Kaiser and Bond, 1959) as determined by Fourier transform infrared spectrometry (FTIR). Occluding diamonds also exhibit typical deep-mantle carbon isotopic compositions of -5% (e.g., Deines and Wickman, 1985) with the exception of the diamond associated with ruby inclusion BZ214A, which has a lighter isotopic composition (-11.56%) more usually associated with eclogitic mantle parageneses.

The occurrence of ruby within the same diamonds as high alumina pyroxene in conjunction with their association with ferropicroclase establishes a mineral paragenesis and provides evidence that the ruby inclusions have an origin within the lower mantle. Specifically, phase relations with Mg,Al-pyroxene (originally perovskite structured) place their origin within a depth range of $\sim 720\text{--}820$ km depending on ambient temperature (Hutchison et al., 2001). At shallower depths in the lower mantle, the mineral phase TAPP (tetragonal almandine-pyrope phase; Harris et al., 1997) acts as principal Al-host whereas with greater pressure, all Al is able to be accommodated within the perovskite-structured polymorph of Mg,Al-pyroxene (Irfune et al., 1996).

Table 1
Occurrence and associated mineralogy and geochemistry of corundum inclusions in Juina diamonds

Inclusion	Description	Size (μm)	Associated phases	N (ppm) ^a	$\delta^{13}\text{C}$
BZ214A	Bright red	–	None	II	-11.56
BZ241C	Red comp. tip to green bfg. grain BZ241B1	$60 \times 40 \times 30^b$	BZ241A ferropicroclase BZ241B1 and B2 Mg,Al-pyroxene	II	-5.30
BZ241Ac	Red-brown	$30 \times 20 \times 20$	same host as above	II	-5.30
BZ227A	Powder blue vitreous	$300 \times 200 \times 150$	None	II	-4.99 -4.41
BZ228A	White isotropic	$60 \times 30 \times 40$	None	n.d.	n.d.
BZ229B	Light blue	$120 \times 50 \times 40$	None	n.d.	n.d.

comp.—composite; bfg.—birefringent; n.d.—not determined.

Data were from this study and Hutchison et al. (1999). Carbon isotopic composition and FTIR analytical techniques are described in Hutchison et al. (1999).

^a Nitrogen was measured by Fourier transform infrared spectrometry (FTIR); II refers to Type IIa diamond, where N concentration is less than 20 ppm.

^b Ruby portion comprises approximately half of this grain.

3. Additional samples

Carmine-coloured corundums PHN6087/20 were recovered from kimberlite drill cores from Forte à la Corne, Canada. In a different study, diamonds with inclusions of ferropicriase have been recovered from elsewhere in Canada, at Lac de Gras (Davies et al., 1999). Without further inclusions to identify a paragenesis and thus constrain a depth of origin, ferropicriase-bearing diamonds may reflect a deep upper mantle origin (Brey et al., 2003) rather than a lower mantle origin. In any case, however, these diamonds have a likely deep mantle origin and therefore it was considered pertinent to question whether the Forte à la Corne samples also had a similar flavour. These samples were also of interest because of their unusual colouration and compositional zonation. The samples were recovered from heavy mineral separation of in excess of 300 kg of kimberlite borehole cores from the Forte à la Corne kimberlite field. The separation procedure involved jaw and roller crushing, HCl acidification and screening, drying at 105–110 °C, electromagnetic separation and heavy mineral separation using bromoform and clerici solution-thallium formate. Separation and handpicking was overseen by Kevin Leahy (Exploration Consultants Ltd.), Oleg von Knorring (deceased) and P.H. Nixon. One representative sample [PHN6087/20(2) and abbreviated herein to PHN20(2)] was chosen for analysis.

Samples obtained from the University of Arizona Mineral Museum consisted of white corundum from the Rockford Granite, Tallapoosa County, AL (UA3640), which is an s-type felsic plutonic suite (Drummond et al., 1988) and granite intruding, felsite dyke-hosted, light-brown corundum from the Sacatan Mountains, Pinal County, AZ (UA12976 of the type recorded in Larrabee, 1969). Claret-coloured corundums var. ruby associated with clinozoisite from Kenya (UA9997) and from high-grade Proterozoic orthoamphibolites of the Bamble Sector, Froland, Arundel, Norway (UA1855 of the type described by Vissor and Senior, 1990; Nijland et al., 1993) were obtained from the same source.

Claret-coloured corundum associated with clinozoisite from Tanzania (PHNz) was provided from the collection of P.H. Nixon in addition to synthetic corundum (SYNCOR) manufactured commercially

by the reaction of chromite with metallic Al to form Cr-corundum plus Cr metal and catalysed with undisclosed Ca- and K-bearing compounds. A synthetic ruby (BURM), believed to be from Burma and obtained in Kuala Lumpur, was also obtained for study.

High-grade granulite-facies hosted samples from Japan and Antarctica were included from the collection of S.L. Harley. The Japanese sample (HIGO) is from Zone D of the Higo Mesozoic metamorphic belt, which is part of the high T/low P Ryoke Belt in Kyushu. The sample is from a high-temperature reaction zone intimately associated with an ultramafic sliver interpreted as being a high-temperature intrusion (800 °C, 5–6 kbar; Osanai et al., 1996). This metasomatised corundum is associated with pale blue Mg-sapphirine, spinel and altered plagioclase. Sample 91–38 (Harley, 1998) is from a garnet sillimanite phlogopite gneiss where corundums are surrounded by coronas of sillimanite, sapphirine and cordierite and constitutes a metasomatic zone between mafic and pelitic rocks hosted in Archaean (2800 Ma) orthogneisses. The remaining samples are all from the Taynaya supracrustals of the Vestfold Hills, Antarctica (Snape and Harley, 1996); samples (65178, 65305 and SH-9296) all come from what are termed ‘Type II’ white sugary textured boudin cores containing assemblages of K-feldspar, corundum, sapphirine and sillimanite. The protoliths are thought to be pyrophyllite or muscovite-bearing rocks, probably claystones of hydrothermally altered clay/sericite/chlorite rocks and are hosted in 2520–2500 Ma TTG suite orthogneisses or as rafts in 2500–2486 Ma monzodioritic gneisses. Sample 65305 was obtained from locality B of Harley (1993), sample 65178 from locality A and sample SH-9296 from within Crooked Lake Gneisses approximately 3 km to the northwest.

4. Inclusion release

It is a significantly delicate task to break diamond samples and retrieve included phases relatively intact and there exists a risk of missing useful inclusion fragments in the resulting residue. However, given the advantages that the retention of diamond hosts for separate analysis provide, in addition to the risk of sample alteration by heating, inclusion release by

fracturing was preferred over burning. Although previously published work has employed similar techniques for inclusion release and sample preparation, a description of the technique has not been widely available and is hence discussed in the following.

An 80/80 stainless-steel anvil housing was employed with a flat base and two removable glass viewing windows toughened with nail polish on either side of the anvils. The anvils, made from hardened silver steel, lie vertically within the housing with the lower anvil being static and the upper anvil being driven by a screw through the top of the housing. The junction between the upper anvil and screw is occupied by a ball bearing to minimise torque. Diamond samples were placed on the static anvil in such a fashion to exploit diamond cleavage planes and to protect the inclusion. Stones occasionally prove to be very hard to break and fractured explosively. To minimise inclusion fracturing, pressure was increased slowly whilst observing the stone by optical microscope. Close to final fracture, energy was often released in the form of high-pitched sound waves and an iridescent interference pattern developed.

Broken material was subsequently brushed into a flat-based petri dish. Potential inclusion grains were measured against a graticule and transferred by wooden needle with finger or silica grease to a lightly greased, glass slide. A ring of epoxy was smeared around the inclusion with a small trail being taken over the inclusion to minimise inclusion movement and the formation of air bubbles on addition of more epoxy. A brass cylinder (~ 4-mm diameter) was then coated internally with epoxy and placed over the inclusion. Small amounts of epoxy were then bled down the inside surface of the cylinder and allowed to harden overnight. To bring the inclusion to the surface, the dried sample was carefully ground to 1/4 µm with diamond grit. Denture fixative (Stachel, personal communication, 1997) can be used rather than epoxy, which although more difficult to handle can reduce sample rounding during polishing.

5. Analytical methods

SIMS was chosen as the most suitable technique for characterisation of the sometimes sub-ppm level quantities of trace elements in unknown corundums.

The ~ 20-µm beam size was considered particularly suitable for analysis of inclusions in diamonds, given their rarity and small size.

Analyses were conducted on inclusions in diamonds using the Cameca ims-4f of the University of Edinburgh/NERC using the duo-plasmatron O⁻ source. An 8nA beam current was used with a contrast diaphragm of 150 µm, field aperture setting of 1 and an energy offset of 80 V. Masses ⁴⁰Ca, ⁴⁸Ti, ⁵²Cr, ⁵⁶Fe, ⁵⁸Ni, ⁶⁹Ga, ⁷⁴Ge, ⁸⁵Rb, ⁸⁸Sr, ⁸⁹Y, ⁹⁰Zr and ²⁰⁸Pb were measured as single positively charged ions, backgrounds were measured at mass 130.5 and high mass standardisation was carried out on ¹⁹⁷Au. Because of the high abundance of mono-isotopic Al, measurement was made at mass 13.5 corresponding to Al²⁺. A ratio of Al²⁺ to Al⁺ of 0.00125 based on Faraday Cup measurement was used in standardisation. Additional corundums, including the standard described in the following, were measured using similar techniques on the Cameca ims-3f of Arizona State University (ASU) and using a 12.5-kV duo-plasmatron source and for masses ²⁴Mg, ²⁸Si, ⁵⁵Mn, ⁶³Cu, ⁸⁵Rb, ⁹³Nb, ⁹⁵Mo, ¹⁰¹Ru and ¹¹⁴Cd in addition to those listed previously. Contrast aperture of 150 µm, field aperture of 1800 µm and energy offset of 75 V were employed.

To fully deconvolute SIMS analysis of unknowns, ion yield values relative to a known element are required. Such values are ideally obtained for standard materials as similar in major element composition and crystal structure to the unknown as possible. For the purposes of this study, a doped Al₂O₃ standard would have been ideal; however, given the absence of historical SIMS analyses of corundums, such standards were not available. Given the difficulty in manufacturing Al₂O₃ glass, eutectic La-aluminate of composition La₃Al₅O₁₂ was chosen as a suitable compromise material with a dominance of Al₂O₃ and comparable structure to corundum. The standard material was prepared as a finely ground powder of oxides of the following elements: La, Al, Si, Cd, Pb, Y, Sr, Ca, Ge, Zr, Nb, Ga, Mg, Mo, Ti, Cu, Ru, Cr, Ni, Mn, Rb and Fe with minor elements introduced as 2000 ppm atomic. Glasses were manufactured by levitation laser vitrification where initial sample chips were fused and heated in an insulating environment held in place by tetrahedrally orientated refractory gas jets. Doping elements were chosen so as to

avoid molecular and ion interferences on SIMS analyses and X-ray overlapping on EPMA. A number of intense green glasses were formed, of which two glasses (1 and 5) were chosen that showed good visual microscopic homogeneity. These samples were characterised by 25 EPMA spot analyses and two line transects on each grain that showed the samples to be closely homogeneous within analytical error for most elements. Most elements were found in concentrations between 50 and 3000 ppm atomic depending on the degree to which the oxides volatilised or were concentrated during manufacture of the glass. Elements Y, Mo and Ru were found to be below detection limit of EPMA analysis and Rb was not measured due to lack of appropriate standards. To optimise the usefulness of the standard glasses, measurements were also conducted using laser inductively coupled plasma mass spectrometry (laser-ICPMS) at the Australian National University's RSES. Five analyses were conducted on each glass by measuring background first and standardising against SRM 610 glass. ^{27}Al was chosen for internal standardisation. As with EPMA measurements, analyses were found to be closely similar within each grain and similar concentrations and depletions of doped elements were usually obtained. Some discrepancies were observed for Si, Cr, Ge, Y and Pb between laser-ICPMS and EPMA analyses. Careful consideration was therefore given to which data to use to represent the best approximation to the standard glass compositions. Broadly, ICPMS analyses were chosen due to superior detection limits although consideration was also given to possible laser-ICPMS interferences and standard deviations of analyses. Preferred average compositions as elemental wt.% for each standard glass are available in Table 1 of the supplementary data set.

Relative ion yield (RIY) values were subsequently calculated from isotope-corrected SIMS measurements of counts per second conducted on both glasses at ASU under the conditions described above and using Al concentrations determined by EPMA. Typically, RIY is expected to be roughly linearly related to first-order ionisation energy and most elements give a good correlation. The obvious outlier is Pb, and given the very low concentration of this element in the standard glass, a RIY value was

estimated to intercept the relationship with ionisation energy of the other elements. RIY values were similarly calculated for Ru and Rb, which were not measured in the standard glasses. Values for RIY are presented in Table 2 of the supplementary data set. Given the close proximity of composition and RIY values of both glasses, averaged data were used for conversion of isotope-corrected cps data for unknowns. RIY values calculated show a good approximation to those obtained during routine SIMS analyses of glass and crystalline standards.

6. Results

All elements were detected in measurable quantities in both natural and synthetic samples with a few exceptions—notably Ru in BURM and Y, Rb and Ru in the low-K portions of PHN20(2). Averaged concentrations for each sample are presented in Table 2 as ppm weight and arranged broadly according to corundum varietal type. Observations are made in the following, where it should be noted that varietal classifications do not follow gemological criteria but are based principally on sample colouration. It is particularly noticeable from Table 2 that corundums that can be broadly classified by colouration show strong similarities of composition, which are distinctly different from corundums of other varieties. Further and as detailed below, corundums from widely differing geographical settings yet similar geological settings are often indistinguishable from each other. All corundums have significant Fe concentrations (≥ 2000 ppm), intermediary Mg and Si (~ 10 – 1000 ppm) and are low in Ca (< 10 ppm). However, rubies and sapphires both have intermediary Ti contents but are, respectively, enriched and depleted in Cr. White sapphires contain intermediate concentrations of Cr and are also more enriched in Ti.

6.1. Ruby-type corundums

Concentrations of trace elements in ruby inclusions from Juina diamonds are presented in Fig. 1. Comparison with rubies from other localities (Fig. 2; Table 2) shows that ruby inclusions are particularly identifiable by high Ni concentrations (18–101 ppm)—often two orders of magnitude greater than other rubies (0.32–

Table 2
Compositions of corundums as determined by SIMS expressed as ppm weight

	BZ227A	65178	SH-9296	91-38	BZ228A	BZ229B	UA12976	HIGO	UA3640	65305	BURM	BZ214A	BZ241Ac	BZ241C	UA1855	PHNz	UA9997	SYN-Hi-K	PHN20-Hi-K	SYN-Lo-K	PHN20-Lo-K
<i>n</i>	2	2	2	2	2	1	2	2	3	2	2	1	1	1	2	2	2	1	1	1	1
**	Blue-D	M/M	M/M	M/M	Wh-D	Wh-D	LBr-Ig	M-Ig	Wh-Ig	M/M	Red-Syn	Ruby-D	Ruby-D	Ruby-D	Ct-M/M	Ct-M/M	Ct-M/M	Br.Red-Syn	Carm-Syn?	Br.Red-Syn	Carm-Syn?
Al	522 400	525 500	523 400	526 100	528 200	524 200	521 600	526 313	522 200	526 600	526 500	476 400	524 000	473 000	522 400	523 300	522 500	430 500	466 300	522 200	511 300
Mg	873.4	93.34	82.43	49.26	<i>201.0</i>	615.1	158.8	170.9	108.2	137.9	5.46	<i>2426</i>	n.d.	<i>2629</i>	39.82	20.98	16.48	897.4	707.8	15.40	14.49
Si	<i>1792</i>	108.1	85.84	148.1	<i>bdl</i>	245.4	318.3	286.2	330.7	168.8	90.02	<i>2732</i>	n.d.	<i>3664</i>	452.8	136.8	301.4	1711	1717	2857	2584
Ca	2.84	1.33	2.67	3.411	1144	3816	4.78	2.04	6.63	9.74	4.83	13.42	132.1	120.6	3.36	2.85	4.76	346.2	1309	3.102	8.032
Ti	414.7	159.2	134.2	63.00	1181	11290	7556	3199	1114	100.0	26.03	355.4	46.05	328.2	69.12	35.02	15.08	20.97	14.82	3.87	3.064
Cr	9.80	32.32	82.62	87.11	534.9	135.3	710.9	97.02	1106	3.48	2933	49960	5630	92 180	5926	5023	5281	28 090	12965	6895	5376
Mn	<i>28.16</i>	0.12	0.10	0.07	<i>bdl</i>	<i>bdl</i>	1.50	13.20	0.60	104.6	0.15	<i>307.3</i>	n.d.	<i>492.2</i>	0.32	0.09	0.20	23.39	8.00	0.68	1.06
Fe	3128	4090	6527	3245	1729	418.0	4083	2309	6677	2952	5.51	1557	175.6	9497	1405	2239	1878	6.95	136.5	0.40	0.65
Ni	36.79	0.42	0.50	0.41	171.2	40.85	0.71	0.34	0.81	2.75	0.33	43.96	18.16	101.1	1.479	0.33	0.45	1.75	12.09	0.34	1.04
Cu	n.d.	14.84	6.65	8.31	n.d.	n.d.	299.2	129.2	46.28	10.35	7.97	n.d.	n.d.	n.d.	6.62	5.99	8.31	4.72	13.18	2.57	8.76
Ga	181.9	36.82	12.30	24.21	1.18	29.44	122.3	38.49	21.17	11.16	1.29	42.12	13.26	62.76	24.13	12.14	9.65	11.31	6.61	1.46	1.37
Ge	198.5	20.48	29.66	13.57	44.96	742.2	110.1	72.23	80.13	67.20	6.49	178.6	3.22	152.3	10.58	11.67	10.05	6.71	1.83	4.09	5.77
Rb	0.03	0.02	0.03	0.03	0.60	2.37	0.03	0.03	0.06	0.12	0.02	0.03	0.07	0.12	0.01	0.01	0.03	1.54	1.25	0.03	<i>bdl</i>
Sr	0.01	0.01	0.02	0.01	2.38	248.8	0.04	0.03	0.30	0.04	0.02	0.04	0.21	0.03	0.02	0.02	0.02	7.99	3.92	0.00	0.01
Y	0.02	0.02	0.01	0.01	0.40	83.28	0.11	0.36	0.01	0.44	0.01	0.00	0.02	0.02	0.00	0.01	0.01	0.08	0.01	<i>bdl</i>	0.01
Zr	0.01	0.01	0.02	0.04	32.37	4403	36.14	1.53	0.02	0.04	0.04	0.06	0.86	0.53	0.01	0.01	0.02	3.36	0.06	0.04	0.02
Nb	0.01	0.03	0.01	0.02	5.57	1.11	22.63	17.92	0.04	0.03	0.05	0.03	0.18	0.18	0.04	0.01	0.03	0.07	0.04	0.01	0.03
Mo	n.d.	0.07	0.12	0.12	n.d.	n.d.	4.81	1.04	0.15	0.12	0.24	n.d.	n.d.	n.d.	0.16	0.27	0.31	0.99	0.41	0.36	0.22
Ru	n.d.	0.05	0.06	0.05	n.d.	n.d.	0.16	0.12	0.05	0.05	<i>bdl</i>	n.d.	n.d.	n.d.	0.17	0.11	0.056	0.029	<i>bdl</i>	0.08	0.07
Cd	n.d.	2.31	3.49	1.74	n.d.	n.d.	11.15	5.62	2.93	2.21	3.25	n.d.	n.d.	n.d.	2.06	2.01	1.05	1.42	2.59	1.31	2.07
Pb	0.45	0.33	0.36	0.42	30.07	3.76	0.58	0.75	0.42	1.26	0.51	1.15	1.73	2.90	0.46	0.37	0.42	0.16	1.16	0.28	0.545
<i>Cr/Ni</i>	0.27	77.49	165.1	211.2	3.12	3.31	994.7	287.6	1372	1.27		1136	310.05	912.03	4008	15 450	11 770	Synthetic	Synthetic?	Synthetic	Synthetic?
<i>Al/Ga</i>	2872	14 270	42 560	21 730	446 300	17 800	4265	13 670	24 660	47 180		11 310	39 520	7537	21 650	43 120	54 150				

ppm values in italics were determined by EPMA; accuracy of sup-ppm analyses are about ± 30% and ppm level analyses range from ± 5% to 20%; n.d.—not determined; *bdl*—below detection limit; SYN—sample SYNCOR; *n*—no. of analyses; **—sample descriptions; D—inclusion; M/M—metamorphic; Ig—igneous; Syn—synthetic; Wh—white; LBr—light brown; Ct—claret; Br.Red—brown red; Crm—carmine; M-Ig—meta-igneous.

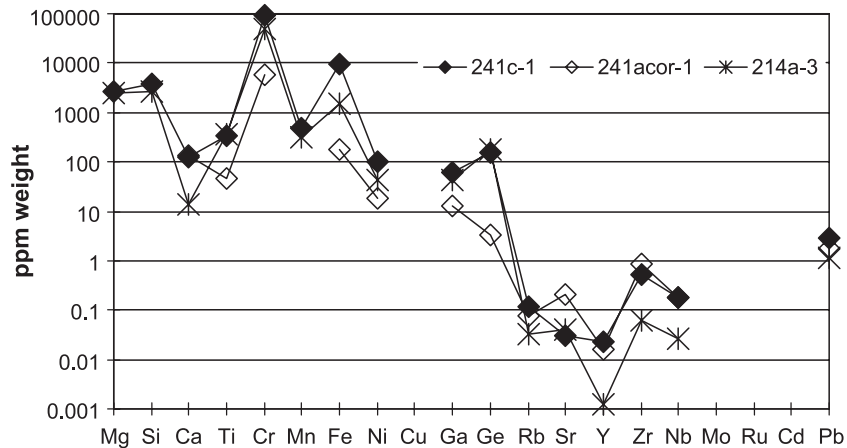


Fig. 1. Concentrations of minor and trace elements in inclusions of ruby from Juina diamonds expressed in ppm weight. Analyses are particularly distinguishable from rubies and corundums from other localities by high Ni concentrations.

1.5 ppm). [Kerrick et al. \(1987\)](#) report high Ni (up to 2000 ppm) in analyses of “corundum”; however, these figures come from neutron activation whole-rock analysis of massive corundums associated with rutile and chlorite. As the same ‘corundums’ are reported to contain upwards of 2 wt.% TiO_2 , it is concluded that these unusual Ni values arise from included phases. Throughout the literature, the highest Ni concentrations reported by precision techniques for natural non-diamond inclusion corundums are from sample 65305 of the current study (2.75 ppm). Juina ruby inclusions are also less evolved having high Mn and ratios of Mg/Fe by weight of 0.27–1.56 compared to 0.008–0.028

for clinozoisite associated rubies and 0.012–0.084 for other natural corundums. It is also notable that notwithstanding the large uncertainties associated with EPMA analyses of minor elements in corundum, analyses that are reported for corundums associated with kimberlites ([Exley et al., 1983](#); [Mazzone and Haggerty, 1989](#)) show intermediary ratios of Mg/Fe ranging from 0.07 to 0.24.

Analyses of samples UA9997, UA1855 and PHNz show closely similar compositions as demonstrated in [Fig. 2](#) to the point of being almost indistinguishable within analytical error. As with ruby inclusions, HFSE and LILE concentrations are low (~ 0.01 – 0.03 ppm).

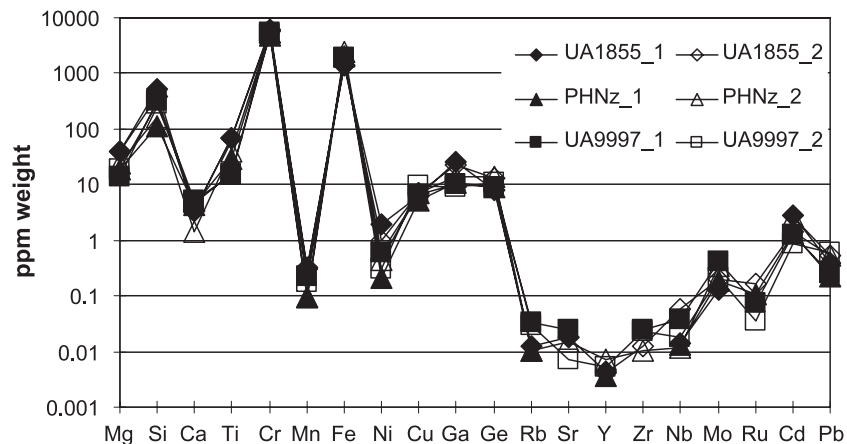


Fig. 2. Concentrations of minor and trace elements in rubies associated with clinozoisite from meta-basic rocks from Norway (UA1855), Kenya (UA9997) and Tanzania (PHNz). The three samples from widely differing geographical origin are strikingly similar in composition.

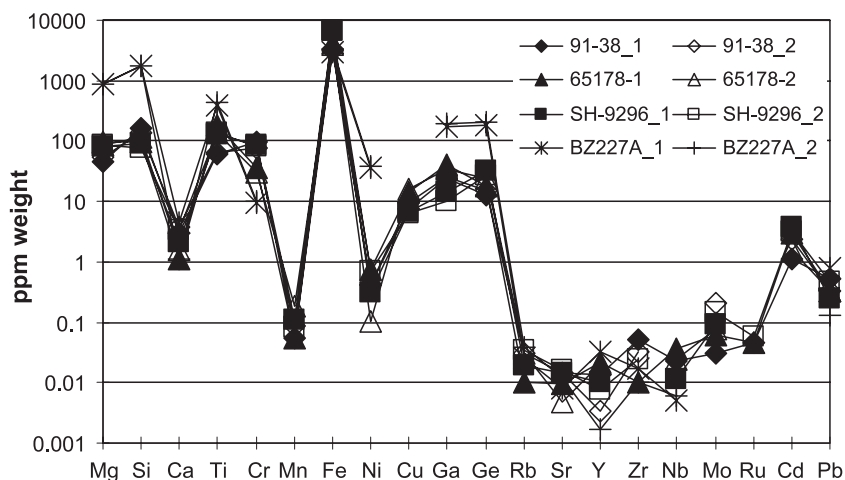


Fig. 3. Concentrations of minor and trace elements in sapphire inclusion BZ227A in comparison with samples 91-38, 65178 and SH-9296 from Antarctic granulites. The inclusion is distinguishable by elevated Ga, Ge and Ni and depleted Cr.

6.2. Sapphire-type corundums

The large, blue sapphire inclusion BZ227A distinguishes itself from other corundums in particular by high Ga and Ge (Fig. 3). It contains ~ 200 ppm weight for both elements compared to tens of ppm for metamorphic origin grains and ~ 100 ppm for igneous sourced samples. Ga concentration data is also available for a small number of gem-quality sapphires from Thailand (Limtrakun et al., 2001) and elsewhere (Emmet et al., 2003). With concentrations ranging from 29.6 to 187.5 ppm weight, these sapphires are intermediate in Ga concentration between the more Ga-rich Juina sapphire inclusions and grains in Antarctic granulites (samples 65178, SH-9296, 91-38 and 65305). Thai sapphires have ratios of Al/Ga ranging from 2820 to 6180 in comparison with 2872 for BZ227A and >14000 for granulite-hosted sapphire-type corundums. Ni contents in BZ227A are about two orders of magnitude higher than otherwise broadly similar samples 65178, SH-9296 and 91-38 from Antarctic granulites whereas Cr contents are lower. Furthermore, BZ227A is very impoverished in LILE and particularly in HFSE compared to otherwise similar igneous and meta-igneous associated corundums UA12976 and HIGO.

65305 and UA3640 have slightly unusual compositions compared to other corundums. They seem to

be most closely allied to sapphire-type compositions except that 65305 has high Y, Ga and Ge and Mn is three orders of magnitude greater (consistently ~ 100 ppm in all three analyses) than comparable grains. UA3640 is unusual as Ti and Cr ppm weight concentrations are almost equal and some analyses show relatively high Sr (~ 0.5 ppm).

6.3. Other natural corundums

White corundum inclusions in Juina diamonds are particularly striking in comparison with all other natural corundums analysed by their relatively high abundances of Ca (>1000 ppm), high field strength elements (HFSE) Y, Zr and Nb and large ion lithophile elements (LILE) Rb and Sr. The closest other sample in terms of HFSE is the felsite-dyke occluding UA12976, which is still significantly depleted in Y. White corundum inclusions are relatively Fe-poor (~ 400–1700 ppm weight) compared to similarly coloured samples that typically contain ~ 3000–7000 ppm weight. In contrast, Mg contents as determined by separate EPMA analysis are high (MgO of ~ 200–600 ppm weight compared to ~ 100–150 ppm weight). Like all the other corundum inclusions in diamonds analysed, Ni contents in white corundums are significantly higher than corundums from other localities. The two inclusions analysed yielded 171.2 and 40.85 ppm weight whereas the highest non-Juina

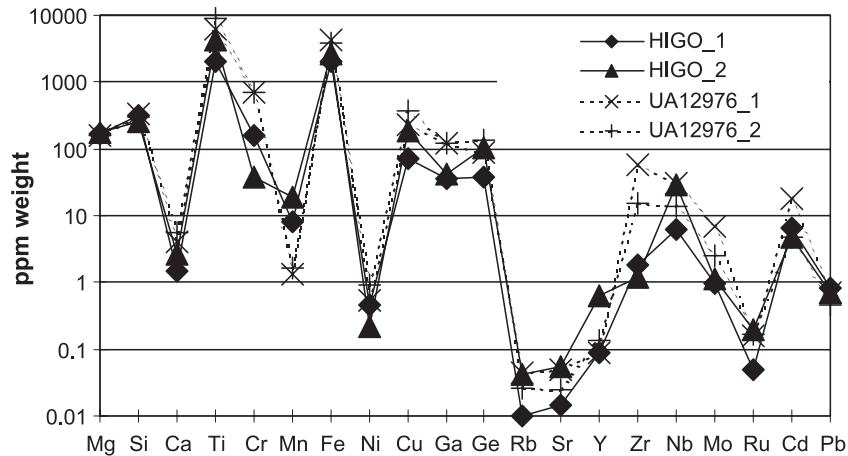


Fig. 4. Concentrations of minor and trace elements in corundums from high-temperature reaction zone associated with ultramafic intrusion from Japan (HIGO) and felsite dyke associated with granite from Arizona (UA12976).

corundum (sample 65305) yielded 2.75 ppm weight. Notably, sample UA3640, which exhibits some characteristics similar to sapphires, shares the characteristic of white corundum inclusions in diamonds in that Ti and Cr have almost equal ppm weight concentrations (~ 1000 ppm).

HIGO and UA12976 show broadly similar compositions (Fig. 4) and are particularly characterised by low (<0.1 ppm) LILE, intermediary Y (~ 0.1 ppm) and high HFSE concentrations (~ 10 ppm).

6.4. Synthetic corundums

SYNCOR and PHN20(2) and other associated grains from PHN6087/20 all show complex intergrowths of regions of varying mean atomic number under back-scattered electron imaging. In contrast, no compositional inhomogeneity was observed for any natural corundums. Analysis by EPMA shows that these zones can broadly be classified into high K and low K. The high-K portions of SYNCOR and

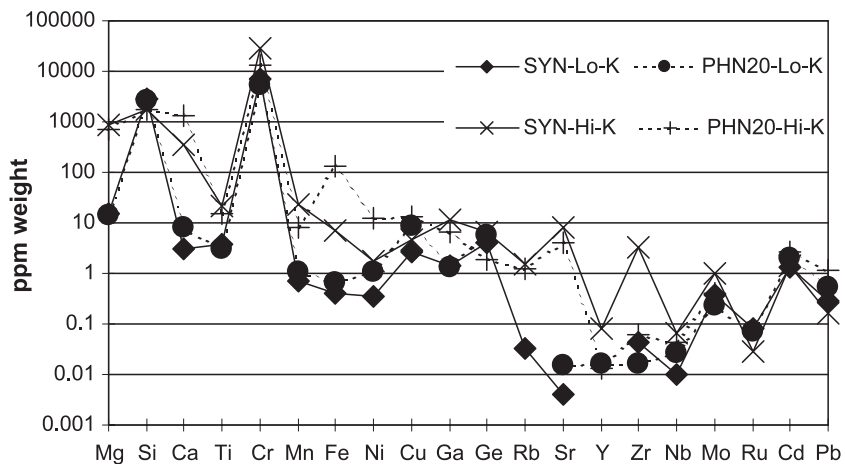


Fig. 5. Concentrations of minor and trace elements in the two principal compositional subdivisions (high and low K) of synthetic corundum (SYNCOR) manufactured by reaction of chromite with metallic Al and PHN20(2) carmine corundum obtained from heavy mineral separate PHN6087/20 from Forte à la Corne kimberlitic drillcore. Both composition of subdivisions and textural characteristics of the two samples are closely similar.

PHN20(2) contain 12.02 and 7.10 wt.% K₂O, respectively, as determined by EPMA analyses and these regions of SYNCOR also contain measurable Na₂O (0.15 wt.%). High-K regions are also distinguishable by relative enrichment in Ca, Fe, Mg and Sr. Low-K regions in SYNCOR and PHN20(2) contain ~ 50 ppm of K₂O. PHN20(2) additionally contains zones containing 25.12 wt.% Cr₂O₃, and 4.72 wt.% CaO, which were too narrow to be measured by SIMS. As can be seen from Table 2 and Fig. 5, equivalent zones in SYNCOR and PHN20(2) are extremely similar in composition with only relatively minor differences between Fe, Ni, Zr and Pb (SYNCOR is relatively deficient in Fe, Ni and Pb and enriched in Zr). Furthermore, synthetic gem ruby BURM, although containing different concentrations of Si, Ti and Fe to low-K zones in SYNCOR and PHN20(2), shows strongly similar HFSE, LILE, Cu, Cd, Pb, Ga and Ge concentrations. It is notable that Ga and Ge in SYNCOR, PHN20(2) and BURM are lower than any natural sample with the marginal exceptions of Ga in BZ228A and Ge in BZ241C.

7. Discussion

The relative abundance of Cr compared to Ti appears to be the most likely influence on the colouration of corundums where the relative quantity of blue-light-absorbing Cr dictates the colouration of rubies and blue-sapphire varieties. Whereas the particularly high abundance of Ti in white corundums contributes to an almost equal absorption across the visible spectrum. More subtle effects are likely due to variable quantities of Fe and trace elements as described by Emmet et al. (2003).

7.1. Origin of corundum inclusions in diamonds

The Ni content of all corundum inclusions typically being orders of magnitude higher than corundums from shallow-sourced settings is regarded as a reflection of the mantle source of the corundum inclusions. Similar arguments are used to support deep mantle sources for ferropericlasite and olivine (0.30–0.41 wt.% NiO) within Juina diamonds (Hutchison, 1997) and elsewhere (Brey et al., 2003). With the exception of one very Fe-rich ferropericlasite outlier, NiO contents vary from 0.3

to 1.49 wt.% with high Ni corresponding to high Mg content. Furthermore, ferropericlasite BZ241A associated with ruby inclusions BZ241C and BZ241Ac contains the highest concentration of Ni observed amongst the Juina suite. The high Mg/Fe ratios observed in Juina rubies are thus consistent with the compositions of Ni and Mg in associated ferropericlasite, further supporting a syngenetic origin of the mineral association.

Ruby inclusions

Ga is frequently associated with Al in rocks and minerals and the ratio of Ga to Al is used as an indication of mantle affinity (Schreyer et al., 1981). Schreyer et al. (1981) attribute the very low Ga/Al ratio measured in corundum-fuschite rocks associated with meta-ultramafics from southern Africa to be a reflection of the unusually high-pressure origin of the rocks they describe. Other ruby samples in the literature from likely crustal rocks (Emmet et al., 2003) have higher Ga concentrations and correspondingly higher Ga/Al ratios.

Although phase relation arguments already place the origin of diamond BZ241 within the lower mantle (Hutchison et al., 2001), low Ga/Al ratios in Juina ruby inclusions in comparison with rubies from other localities and ratios of Mg/Fe higher than those recorded from xenoliths in kimberlites (Exley et al., 1983; Mazzone and Haggerty, 1989), which in turn are higher than crustal samples, lend further support to a mantle origin.

Sapphire inclusion

Following the arguments above, the particularly high abundance of Ga in sapphire inclusion BZ227A is also consistent with a mantle origin. With the exception of association with diamond, which places the origin of BZ227A at greater than ~ 80 km, the absence of other associated mineral phases precludes the use of phase relation arguments to shed further light on a depth of origin. However, as phase relation and other arguments for additional Juina corundum inclusions place their origin within the lower mantle, a deep mantle origin for BZ227A would not be considered unlikely. Furthermore, Limtrakun et al. (2001) link the compositions of their gem-sapphire samples to formation in K- and CO₂-rich alkali magmatism. Given that their Ga concentrations are not as high as

those of BZ227A, this observation is considered to lay further weight to a deep magmatic origin for the Juina sapphire inclusion. Additionally, inclusion study and measurement of nitrogen characteristics (Hutchison et al., 1999) in run-of mine production of Juina diamonds are compatible with the majority of diamonds being of transition-zone and lower-mantle origin. Lower mantle origin diamonds besides having carbon isotopic compositions of $\sim -5\%$ are also almost exclusively Type IIa (Hutchison et al., 1999). As Table 1 shows, similar measurements were obtained for diamond BZ227; hence, again, the evidence is at least consistent with a lower mantle origin for sapphire BZ227A.

Other corundum inclusions

The relatively high Mg contents over Fe in white corundum inclusions in diamonds compared to similar corundums from other sources would point to a more mafic origin. This observation would appear to be at odds, however, with the large abundance of volatile elements. Given the association with diamond, it would appear likely that corundum inclusions of this type would have formed from a partially fluid phase responsible for the syngenetic formation of diamond. This fluid could conceivably act as a carrier for volatile elements of the type observed. However, it is not generally held that LILE are associated with diamond formation from other localities. In addition, LILE concentrations in other Juina inclusions are unremarkable and it is only notable that Zr and Nb in Juina rubies are somewhat elevated above rubies from other localities. In the absence of associated mineral phases by which to estimate pressure and temperature conditions of origin, geochemical indicators are used to support a preferred model that the Juina white corundum-occluding diamonds were formed at shallower depth than Juina ruby inclusions, still within the mantle but involving a more significant crustal component.

7.2. Other natural corundums

The high concentrations of highly mobile HFSE seen in corundums associated with magmatic metasomatism (HIGO and UA12976) is not surprising considering the likelihood of high concentrations of these elements in metasomatising fluids. Metamor-

phism of the HIGO sample may have further contributed to this aspect of its composition. The unusually high Mn concentration of sample 65178 is most likely a reflection of the metamorphic host's claystone protolith.

7.3. Synthetic corundums

The occurrence of the same types of zonation with very strongly similar compositions between synthetic corundum SYNCOR and PHN20(2) is striking given the differing sources for the two samples and especially as sample PHN20(2) was originally considered to be a natural constituent of the manual disintegration of kimberlitic core. Furthermore, all of SYNCOR, PHN20(2), synthetic gem ruby (BURM) and synthetic ruby and sapphire of Emmet et al. (2003) have unusually low concentrations of Fe, Ti and Ga compared to natural rubies, strongly suggesting that PHN20(2) also has an artificial origin. Although mineral separation from core was conducted carefully and corundum was not understood to have been a constituent of the drilling process, neither its use nor its existence as a contaminant can be totally excluded.

8. Conclusions and possible applications

As corundum is shown to occur syngenetically with diamond and its hardness and chemical stability lend it to survival in conditions more extreme than other diamond-associated minerals, potential exists for corundum to be used as a tool for diamond prospectivity. We have demonstrated with a small sample set that minor and trace element compositions of corundum show strong similarities amongst corundums from related geological yet varied geographical settings. At the same time, identifiable differences occur between corundums from differing geological settings and in particular corundum inclusions in diamonds are shown to be distinguishable from other samples. In this case, all inclusion corundums, namely sapphire, ruby and white corundum, are particularly identifiable by high Ni concentrations in excess of 20 ppm; at least an order of magnitude greater than Ni in other samples and large ratios of Mg relative to Fe. Additional precision would be achieved by expanding the present data set into more

samples and a larger range of geological settings. At this stage, the data indicates that mantle-sourced corundums are separable from crustal corundums. Corundums are reported from mantle rocks (notably Padovani and Tracey, 1981; Exley et al., 1983; Mazzone and Haggerty, 1989; Rossman and Smyth, 1990) although trace element data have not been obtained. Opportunity exists therefore for an expanded trace element study involving more mantle material where it is hoped that subdivision within the mantle could be achievable.

As corundum is a common accessory phase in rocks from a range of geological settings, it is envisaged that corundums with a diamond association may often be significantly outnumbered by those from nondiamond-bearing country rocks. At this stage, application as a prospecting tool would encounter limitations; however, it is likely that high Mg/Fe ratios could be easily detectable by rapid energy dispersive spectrometry (EDS) techniques such as currently being developed by Australia's CSIRO and the Geological Survey of Denmark and Greenland. Furthermore, elevated Ni concentrations may also be detectable by these techniques and certainly suitable samples should be rapidly identifiable by laser-ICPMS and with minimal sample preparation. Once suitable grains are identified, fully quantitative analyses could then be achieved. It is therefore envisaged that corundum has potential to be developed as a tool to compliment conventional indicator mineral techniques in diamond prospectivity.

Acknowledgements

Mimi Hill (University of Liverpool), Peter Gummer and the Rhonda Mining, Shirley Wetmore (University of Arizona), Sopemi and the DTC are thanked for supply of samples. Martin Wilding (Arizona State University) is acknowledged for advice on the formulation of standard La-aluminate glass carried out by Jean Tangeman (Containerless Research Inc.). John Craven (University of Edinburgh), Rick Hervig (Arizona State University), Eric Condliffe (University of Leeds) and Hugh O'Neill and Charlotte Allen (ANU) are recognised for analytical support. The work presented in this paper was supported by N.E.R.C. postgraduate funding under

Ben Harte (University of Edinburgh) and Jeff Harris (University of Glasgow), the N.S.F. (EAR 97-06024, 00-01945), an ANU Visiting Fellowship and Diagem International Resources Corp. for conference attendance to M.T.H. This manuscript benefited from the constructive criticism of Julie Hollis (GEUS) and reviews by Steve Haggerty and Craig B. Smith.

References

- Brey, G.P., Bulatov, V., Girmis, A., Harris, J.W., Stachel, T., 2003. Ferropicrinite—a lower mantle phase in the upper mantle. In: Mitchell, R., et al. (Eds.), 8th International Kimberlite Conference Extended Abstracts. On CD-ROM.
- Davies, R., Griffin, W.L., Pearson, N.J., Andrew, A., Doyle, B.J., O'Reilly, S.Y., 1999. Diamonds from the Deep: Pipe DO-27, Slave Craton, Canada. In: Gurney, J.J., et al., (Eds.), Proc. VIIIth Internat. Kimberlite Conf., vol. I. Red Roof Design, Cape Town, pp. 148–155.
- Deines, P., Wickman, F.E., 1985. The stable carbon isotopes in enstatite chondrites and Cumberland Falls. *Geochim. Cosmochim. Acta* 49, 89–95.
- Drummond, M.S., Wesolowski, D., Allison, D.T., 1988. Generation, diversification and emplacement of the Rockford Granite, Alabama appalachians: mineralogic, petrologic, isotopic (C & O) and P–T constraints. *J. Petrol.* 29, 869–897.
- Emmet, J.L., Scarratt, K., McClure, S.F., Moses, T., Douthit, T.R., Hughes, R., Novak, S., Shigley, J.E., Wang, W., Bordelon, O., Kane, R.E., 2003. Beryllium diffusion of ruby and sapphire. *Gems Gemol.* 39, 84–135.
- Exley, R.A., Smith, J.V., Dawson, J.B., 1983. Alkremite, garnetite and eclogite xenoliths from Bellsbank and Jagersfontein, South Africa. *Am. Mineral.* 68, 512–516.
- Gasparik, T., Hutchison, M.T., 2000. Experimental evidence for the origin of two kinds of inclusions in diamonds from the deep mantle. *Earth Planet. Sci. Lett.* 181, 103–114.
- Harley, S.L., 1993. Sapphirine granulites from the Vestfold Hills, East Antarctica: geochemical and metamorphic evolution. *Antarct. Sci.* 5, 389–402.
- Harley, S.L., 1998. Ultrahigh temperature granulite metamorphism (1050 °C, 12 kbar) and decompression in garnet (Mg70)-orthopyroxene-sillimanite gneisses from the Rauer Group, East Antarctica. *J. Metamorph. Geol.* 16, 541–562.
- Harris, J.W., Hutchison, M.T., Hursthouse, M., Light, M., Harte, B., 1997. A new tetragonal silicate mineral from the lower mantle. *Nature* 387, 486–488.
- Harte, B., Harris, J.W., Hutchison, M.T., Watt, G.R., Wilding, M.C., 1999. Lower mantle mineral associations in diamonds from São Luiz, Brazil. In: Fei, Y., Bertka, C., Mysen, B.O. (Eds.), *Mantle Petrology: Field Observations and High Pressure Experimentation: A Tribute to Francis R. (Joe) Boyd*. *Geochem. Soc. Spec. Publ.*, vol. 6. The Geochemical Society, Houston, pp. 125–153.
- Hutchison, M.T., 1997. Constitution of the deep transition zone and

- lower mantle shown by diamonds and their inclusions. PhD Thesis of the University of Edinburgh, p. 660. CD-ROM.
- Hutchison, M.T., Cartigny, P., Harris, J.W., 1999. Carbon and nitrogen composition and cathodoluminescence characteristics of transition zone and lower mantle diamonds from São Luiz, Brazil. In: Gurney, J.J., et al. (Eds.), *Proceedings of the VIIth International Kimberlite Conference*, vol. I. Red Roof Design, Cape Town, pp. 372–382.
- Hutchison, M.T., Hursthouse, M.B., Light, M.E., 2001. Mineral inclusions in diamonds: associations and chemical distinctions around the 670 km discontinuity. *Contrib. Mineral. Petrol.* 142, 119–126.
- Irifune, T., Koizumi, T., Ando, J.-I., 1996. An experimental study of the garnet–perovskite transformation in the system MgSiO_3 – $\text{Mg}_3\text{Al}_2\text{Si}_3\text{O}_{12}$. *Phys. Earth Planet. Inter.* 96, 147–157.
- Kaiser, W., Bond, W.L., 1959. Nitrogen, a major impurity in common type I diamond. *Phys. Rev.* 115, 857–863.
- Kaminsky, F.V., Zakharchenko, O.D., Davies, R., Griffin IV, W.L., Khachatryan-Blinova, G.K., Shiryaev, A.A., 2001. Superdeep diamonds from the Juina area, Mato Grosso State, Brazil. *Contrib. Mineral. Petrol.* 140, 353–374.
- Kerrick, R., Fyfe, W.S., Barnett, R.L., Blair, B.B., Willmore, L.M., 1987. Corundum, Cr-muscovite rocks at O’Briens, Zimbabwe: the conjunction of hydrothermal desilicification and LIL-element enrichment—geochemical and isotopic evidence. *Contrib. Mineral. Petrol.* 95, 481–498.
- Larrabee, D.M., 1969. Corundum. *Mineral and water resources. Bull. Ariz. Bur. Mines* 180, 336–337.
- Limtrakun, P., Zaw, K., Ryan, C.G., Mernagh, T.P., 2001. Formation of the Denchai gem sapphires, northern Thailand: evidence from mineral chemistry and fluid/melt inclusion characteristics. *Mineral. Mag.* 65, 725–735.
- Mazzone, P., Haggerty, S.E., 1989. Peraluminous xenoliths in kimberlite: metamorphosed restites produced from partial melting of pelites. *Geochim. Cosmochim. Acta* 53, 1551–1561.
- Nijland, T.G., Liauw, F., Visser, D., Maijer, C., Senior, A., 1993. Metamorphic petrology of the Froland corundum-bearing rocks: cooling and uplift history of the Bamble Sector, South Norway. *Bull. Norges Geol. Unders.* 424, 51–63.
- Osanai, Y., Hamamoto, T., Kamei, A., Owada, M., Kagami, H., 1996. High-temperature metamorphism and crustal evolution of the Higo metamorphic terrane, central Kyushu, Japan (in Japanese with English abstr.). *Tectonics and Metamorphism. SOUBUN, Japan*, pp. 113–123.
- Padovani, E.R., Tracey, R., 1981. A pyrope–spinel (alkremite) xenolith from Moses Rock Dike: first known North American occurrence. *Am. Mineral.* 66, 741–745.
- Rossmann, G.R., Smyth, J.R., 1990. Hydroxyl contents of accessory minerals in mantle eclogites and related rocks. *Am. Mineral.* 75, 775–780.
- Schreyer, W., Werding, G., Abraham, K., 1981. Corundum–Fuchsite rocks in greenstone belts of southern Africa: petrology, geochemistry, and possible origin. *J. Petrol.* 22, 191–231.
- Snape, I., Harley, S.L., 1996. Magmatic history and the high-grade geological evolution of the Vestfold Hills, East Antarctica. *Terra Antarct.* 3, 23–38.
- Vissor, D., Senior, A., 1990. Aluminous reaction textures in orthoamphibole-bearing rocks: the pressure–temperature evolution of the high-grade Proterozoic of the Bamble sector, south Norway. *J. Metamorph. Geol.* 8, 231–246.
- Watt, G., Harris, J., Harte, B., Boyd, S., 1994. A high-chromium corundum (ruby) inclusion in diamond from the São Luiz alluvial mine, Brazil. *Mineral. Mag.* 58, 490–492.